Special Issue Review Article

IN BIOMEDICINE

Received: 10 December 2010, Revised: 9 June 2011, Accepted: 14 June 2011, Published online in Wiley Online Library: 2011

(wileyonlinelibrary.com) DOI: 10.1002/nbm.1772

^{13}C MRS studies of neuroenergetics and neurotransmitter cycling in humans

Douglas L. Rothman[a,b]*, Henk M. De Feyter[a], Robin A. de Graaf[a,b], Graeme F . Mason[a,c] and Kevin L. Behar[c]

In the last 25 years, ^{13}C MRS has been established as the only noninvasive method for the measurement of glutamate neurotransmission and cell-specific neuroenergetics. Although technically and experimentally challenging, ^{13}C MRS has already provided important new information on the relationship between neuroenergetics and neuronal function, the energy cost of brain function, the high neuronal activity in the resting brain state and how neuroenergetics and neurotransmitter cycling are altered in neurological and psychiatric disease. In this article, the current state of ^{13}C MRS as it is applied to the study of neuroenergetics and neurotransmitter cycling in humans is reviewed. The focus is predominantly on recent findings in humans regarding metabolic pathways, applications to clinical research and the technical status of the method. Results from *in vivo* ^{13}C MRS studies in animals are discussed from the standpoint of the validation of MRS measurements of neuroenergetics and neurotransmitter cycling, and where they have helped to identify key questions to address in human research. Controversies concerning the relationship between neuroenergetics and neurotransmitter cycling and factors having an impact on the accurate determination of fluxes through mathematical modeling are addressed. We further touch upon different ^{13}C-labeled substrates used to study brain metabolism, before reviewing a number of human brain diseases investigated using ^{13}C MRS. Future technological developments are discussed that will help to overcome the limitations of ^{13}C MRS, with special attention given to recent developments in hyperpolarized ^{13}C MRS. Copyright © 2011 John Wiley & Sons, Ltd.

Keywords: ^{13}C; MRS; brain; metabolism; neurotransmitter cycling; human; neuroenergetics

INTRODUCTION

In this article, we review the current state of ^{13}C MRS as it is used to study neuroenergetics and neurotransmitter cycling in humans. We focus primarily on the present status of the measurement (pathways and spatial resolution) and recent findings, leaving descriptions of the experimental protocols and methodology to other articles in this issue. We finish by reviewing the results of the initial applications of ^{13}C MRS and ^{1}H–^{13}C MRS to the study of human disease and potential improvements in the sensitivity, cost and ease of performance of studies.

^{13}C MRS is presently the only method that provides noninvasive measurements of neuroenergetics and neurotransmitter cycling in the human brain. The ability to use ^{13}C MRS to study cell-specific neuroenergetics and neurotransmitter cycling is a result of the localization of key enzymes and metabolite pools in neurons and glia, and the specificity of ^{13}C-labeled precursors to specific cell types. Figure 1 shows a diagram of neuronal and astrocyte (a type of glial cell) cell metabolism and the interplay of neuronal and astrocyte metabolism via the glutamate/glutamine cycle. Both neurons and astrocytes can take up glucose and oxidize it in their mitochondria via the tricarboxylic acid (TCA) cycle. As discussed below, neurons and astrocytes can oxidize lactate and β-hydroxybutyrate in addition to glucose, and astrocytes can also oxidize acetate and fatty acids. Excitatory glutamatergic neurons, which account for over 80% of the neurons and synapses in the cerebral cortex (1), release glutamate as a neurotransmitter, most of which is taken up by astrocytes (2,3) and converted to glutamine or oxidized (4,5). Neurons lack the enzymes required for the *de novo* synthesis of glutamate, and therefore depend on astrocytes to provide substrates for the synthesis of glutamate lost during neurotransmission (6). The neuron then converts glutamine to glutamate via phosphate-activated glutaminase. The complete series of steps from neuronal glutamate release to the resynthesis of glutamate from glutamine is called the 'glutamate/glutamine cycle'.

Figure 2 shows the spectra obtained at 4 T from human brain localized to the midline occipital/parietal lobe during the infusion of three different isotopically labeled substrates: 99%

* *Correspondence to: D. L. Rothman, Magnetic Resonance Research Center, Departments of Diagnostic Radiology and Biomedical Engineering, Yale University School of Medicine, 300 Cedar Street, PO Box 208043, New Haven, CT 06520–8043, USA.*
E-mail: douglas.rothman@yale.edu

a *D. L. Rothman, H. M. De Feyter, R. A. de Graaf, G. F. Mason*
Department of Diagnostic Radiology, Magnetic Resonance Research Center, Yale University School of Medicine, New Haven, CT, USA

b *D. L. Rothman, R. A. de Graaf*
Department of Biomedical Engineering, Yale University, New Haven, CT, USA

c *G. F. Mason, K. L. Behar*
Department of Psychiatry, Magnetic Resonance Research Center, Yale University School of Medicine, New Haven, CT, USA

Abbreviations used: *AV, arteriovenous; $CMR_{glc(ox)}$, cerebral metabolic rate of glucose oxidation; GABA, γ-aminobutyric acid; PC, pyruvate carboxylase; PET, positron emission tomography; RF, radiofrequency; TCA, tricarboxylic acid; V_{cyc}, glutamate/glutamine cycle rate; V_{Gln}, glutamine synthesis rate; V_{PC}, rate of anaplerosis through pyruvate carboxylase; V_{TCAa}, astroglial TCA cycle rate; V_{TCAn}, neuronal TCA cycle rate; V_x, mitochondrial α-ketoglutarate to cytosolic glutamate exchange rate.*

enriched [1-^{13}C]glucose, [3-^{13}C]lactate and [2-^{13}C]acetate. It shows labeling in the brain pools of aspartate, γ-aminobutyric acid (GABA), glutamine and glutamate. The brain pools of glutamate, GABA and glutamine have been shown to be localized within glutamatergic neurons, GABAergic neurons and glia, respectively (under nonpathological conditions). By following the flow of ^{13}C label from glucose, acetate and other precursors into these metabolites, MRS in combination with metabolic modeling allows the measurement of the TCA cycle rate in glutamatergic neurons, GABAergic neurons and glia, as well as glutamate and GABA neurotransmitter cycles between neurons and astrocytes (7,8). When expressed as total substrate oxidation, the rates determined by MRS are found to be in excellent agreement with earlier methods, including positron emission tomography (PET) (7,9–11). However, *in vivo* MRS is unique among other techniques in its measurement of cell type-specific energetics and neuronal/glial neurotransmitter cycles.

STUDIES IN ANIMAL AND CELL MODELS OF THE GLUTAMATE/GLUTAMINE CYCLE AND NEURONAL AND GLIAL ENERGETICS

Although this article primarily focuses on human studies, we briefly review some relevant investigations in animal and cell models which have helped to validate ^{13}C MRS measurements of neuroenergetics and neurotransmitter cycling, as well as to identify key questions to address in human research.

Glutamate neurotransmitter cycling is the main pathway of cerebral cortex glutamine synthesis

Although the metabolic pathways of glial glutamate uptake and the glutamate/glutamine cycle are well established from ^{14}C radiotracer and cellular studies, they were not considered to be relevant to neuroenergetics prior to *in vivo* studies using MRS (4,12,13). Because the neurotransmitter glutamate was shown to be packaged in small vesicles, the predominant concept arose of a small, nonmetabolic 'transmitter' pool which did not interact with the large 'metabolic' glutamate pool (14,15). This concept was brought into question by one of the first ^{13}C MRS studies of human brain (16), which found a high rate of glutamine labeling from [1-^{13}C]glucose in the human occipital/parietal lobe. At the time of the study, it was unclear whether this high labeling was a result of the glutamate/glutamine cycle or of glutamine synthesis to remove ammonia from the brain, the latter believed to be its major role (17). As pointed out by Sibson *et al.* (18) in 1997, these pathways could be distinguished because glutamine that leaves the brain must be replaced by anaplerosis, which occurs in glial cells. Furthermore, because of mass balance constraints, the glutamine synthesized for this purpose must match the efflux of glutamine and uptake of ammonia and CO_2 by the brain, as measured by the arteriovenous (AV) difference (5,18). To distinguish these possibilities, glutamine synthesis was measured in rat cortex during hyperammonemia. When blood ammonia levels were extrapolated to a physiologically normal and low value, anaplerosis was found to account for approximately 20% of glutamine synthesis (18). Measurements of anaplerotic glutamine synthesis using precursors that label this pathway

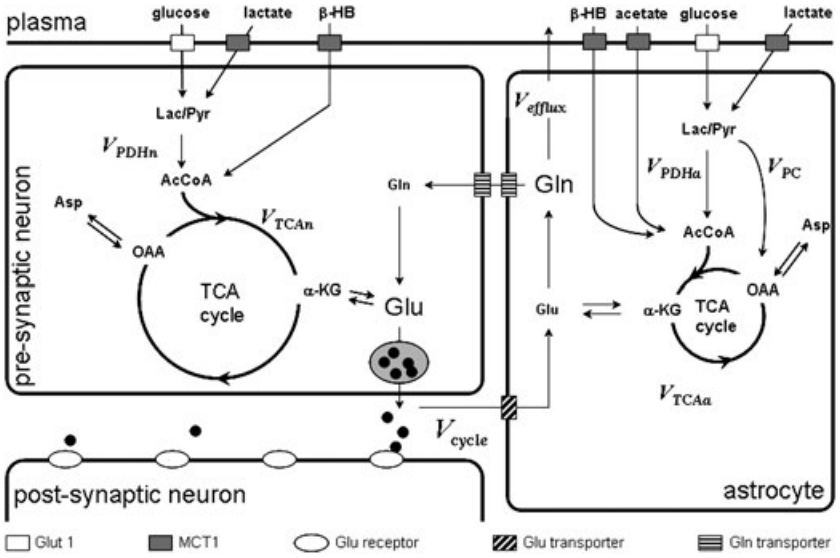

Figure 1. Diagram of the glutamate (Glu)/glutamine (Gln) cycle (V_{cycle}). The diagram shows the metabolic pathways within glutamatergic neurons and surrounding astroglial cells. Glucose and lactate enter both the glial (V_{TCAa}) and neuronal (V_{TCAn}) tricarboxylic acid (TCA) cycles via pyruvate dehydrogenase (V_{pdh}), β-hydroxybutyrate (β-HB) is directly incorporated into the neuronal and astroglial TCA cycles, and acetate is near-exclusively incorporated into the glial TCA cycle. Neuronal Glu that is released via neurotransmission is taken up by astroglial cells and converted by Gln synthetase to Gln at a rate proportional to the Glu/Gln cycle. The synthesis of Gln is believed to be exclusively within astroglia and other glial cells. In addition to neurotransmitter cycling, Gln may be synthesized *de novo* starting with the pyruvate carboxylase (PC) reaction (V_{PC}). Gln synthesized via PC can replace neurotransmitter Glu oxidized in the astrocyte or elsewhere (and be recycled back to the neuron) or leave the brain (V_{efflux}) to remove ammonia and maintain the nitrogen balance (5,17,26). To measure the rates of these pathways, ^{13}C-labeled substrates are used and the flow of ^{13}C isotope into Glu and Gln is measured using ^{13}C MRS. For detailed descriptions of how these pathways are tracked using ^{13}C MRS, and how isotopically labeled substrates and rates are calculated by metabolic modeling, see refs. (24–26,44,45,47,143). AcCoA, acetyl-CoA; Asp, aspartate; Glut 1, glucose transporter 1; α-KG, α-ketoglutarate; Lac, lactate; MCT1, monocarboxylate transporter 1; OAA, oxaloacetate; Pyr, pyruvate.

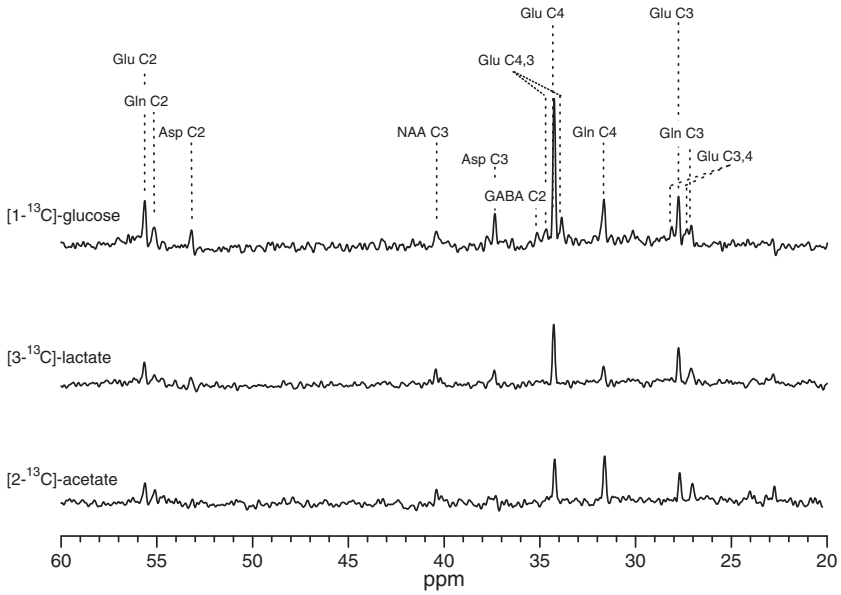

Figure 2. Localized ^{13}C MR spectra acquired at 4 T from the midline occipital/parietal lobe of a volunteer infused with ^{13}C-labeled glucose, lactate or acetate. Top spectrum: acquired during the last 18 min of a 2-h [1-^{13}C]glucose infusion. Middle spectrum: acquired during the last 18 min of a 2-h [3-^{13}C] lactate infusion ($[Lac]_{Plasma}$ ~ 1.5 mmol/L; ^{13}C fractional enrichment ~ 30%). Bottom spectrum: acquired during the last 18 min of a 2-h [2-^{13}C]acetate infusion. Spectra are scaled to *N*-acetylaspartate (NAA) C3 to exhibit the differences in ^{13}C fractional enrichment reached for glutamate (Glu), glutamine (Gln) and aspartate (Asp). The highest fractional enrichment is attained with glucose as label precursor. For glucose or lactate as precursor, the majority of labeling appears in glutamate C4, consistent with the majority of brain metabolism of these substrates occurring in the neurons which contain the majority of glutamate under normal conditions (25). In contrast, label from [2-^{13}C]acetate is highly enriched in glutamine C4, consistent with the localization of acetate metabolism in the astrocyte tricarboxylic acid (TCA) cycle, as shown in Fig. 1, resulting in preferential labeling of glutamine C4. GABA, γ-aminobutyric acid.

directly ([2-^{13}C]glucose, ^{15}N-ammonia and $^{14}CO_2$) have found that approximately 80% of glutamine synthesis is devoted to neurotransmitter cycling (18–22). The analysis of ^{13}C-labeled extracellular glutamate measured by microdialysis and mass spectrometry led to a similar conclusion that neurotransmitter cycling is the major source of glutamine (23). Similar conclusions have been obtained from studies performed in human brain using [1-^{13}C]glucose, [2-^{13}C]acetate and [2-^{13}C]glucose as labeled substrates (24–27).

The glutamate/glutamine cycle is a major metabolic pathway and is directly coupled to neuroenergetics

To determine the relationship between the glutamate/glutamine cycle and cerebral cortex neuroenergetics, ^{13}C MRS was used to measure the relationship between neuronal glucose oxidation and the glutamate/glutamine cycle rate (V_{cyc}) in rat cerebral cortex (28). Cortical activity was modulated through anesthesia ranging from an isoelectric electroencephalograph to higher electroencephalograph activity at two lower doses of anesthesia. With increasing electrical activity, V_{cyc} and the rate of neuronal glucose oxidation via the TCA cycle [expressed as $CMR_{glc(ox)}$ in Sibson *et al*. (29)] increased linearly with a slope of 1.0 ± 0.1. Subsequent studies have confirmed this relationship [see Hyder *et al*. (11) for a review]. Figure 3 shows a plot of measurements in the rat cerebral cortex of the V_{TCAn} plotted *versus* V_{cyc} taken from 11 published research articles at different levels of brain electrical activity ranging from isoelectricity to awake. As reported originally by Sibson *et al*. (29), the relationship between V_{cyc} and $0.5V_{TCAn}$ (where V_{TCAn} is the neuronal TCA cycle rate) is linear with a slope of 0.89 ± 0.06. [We note that, in the article by Sibson *et al*. (29), $0.5V_{TCAn}$ was taken to be equivalent to neuronal glucose oxidation, which would be the case under the hyperglycemic conditions of the study when glucose is the only net fuel for neuronal oxidation (28).] Furthermore, comparison of the intercept at isoelectricity *versus* the values of V_{TCAn} and V_{cyc} in the awake state confirms that over 80% of neuronal oxidative ATP production is coupled to neuronal signaling (as measured by V_{cyc}), even in the absence of stimulation. Thus, V_{cyc} in the awake state is close to the rate of neuronal glucose oxidation and constitutes a major metabolic flux. As described below, recent ^{13}C MRS results from human cerebral cortex are consistent with this finding.

There are several molecular models that have been proposed to explain the near-stoichiometric relationship between changes in the flux of neuronal glucose oxidation and the glutamate/glutamine cycle. The relationship has been shown to be consistent with a model in which the energy for taking up the neurotransmitter glutamate into the astrocyte is provided using glycolytic ATP production from glucose or glycogen (4,30,31). Alternatively, it has been shown that the observed slope can be explained by the redox shuttling requirements between the neuronal cytosol and mitochondria in order to oxidize glutamine taken back up from glial cells (4). The determination of the actual molecular mechanism may have important implications for the understanding of brain disease as any dysfunction in this mechanism would have a severe impact on the ability to sustain neurotransmission. In addition, the measured coupling between neurotransmission and neuroenergetics has provided key data for detailed models of the energy budget of the brain for the support of signaling and information transfer (32–35).

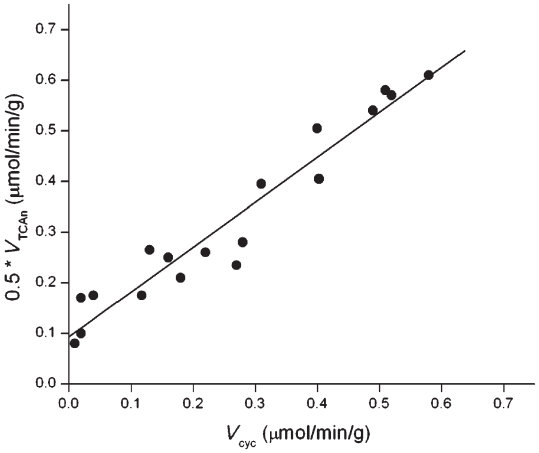

Figure 3. Approximately 1 : 1 relationship between the neuronal tricarboxylic acid (TCA) cycle ($0.5V_{TCAn}$) and the glutamate/glutamine cycle (V_{cyc}) with increasing electrical activity in the rat cerebral cortex. The plot shows the mean values of $0.5V_{TCAn}$ [equivalent to $CMR_{glc(ox)N}$ in Sibson *et al*. (29)] plotted *versus* V_{cyc} reported from 11 published studies at activity levels ranging from awake to isoelectricity (20,22,28,36,39,59,127, 150–153). Regression analysis yields a slope of 0.89 ($R^2 = 0.92$) and an intercept of $0.5V_{TCAn}$ of 0.09 at isoelectricity ($V_{cyc} \sim 0$), values similar to those found in the original 1998 study by Sibson *et al*. (29). In the case of ref. (39), for both the anesthetized and awake states, values of V_{TCAn} were calculated from the time constants reported for glutamate turnover during a glucose infusion. The ratio of glutamate to glutamine steady-state fractional enrichment during [2-^{13}C]acetate infusion was used to calculate V_{cyc} using the equation described in Lebon *et al*. (25).

Validation of measurements of neurotransmitter cycling and anaplerosis using alternative substrates and labeling strategies

A strategy that has been employed to validate glutamate/glutamine cycle measurement is the use of alternative ^{13}C- and ^{15}N-labeled substrates that are incorporated specifically in astrocytes. The subsequent flow of label from astrocyte glutamine (or other potential trafficking substrates) into neuronal glutamate then provides an independent measure of V_{cyc} from studies using [1-^{13}C]glucose, which labels the neuronal glutamate pool to a greater degree than the glial pool. Animal studies employing this strategy have used as label sources ^{15}N-ammonia (27), [2-^{13}C] glucose (5), $^{14}CO_2$ (19,20) and [2-^{13}C]acetate (36–40), and have found results consistent with a high rate of glutamate neurotransmitter trafficking. Similar results have been reported in studies of human subjects using [2-^{13}C]acetate (25,41) and [2-^{13}C]glucose as tracers (26). In addition, the analysis of the ^{15}N labeling of glutamine obtained from extracellular fluid also supported the majority of glutamine being derived from glutamate neurotransmitter cycling (23). In principle, extracellular fluid measurement is a more direct assessment than whole-tissue MRS measurement of the pools relevant to neurotransmission.

In addition to the glutamate/glutamine cycle, there are several other potential pathways of neurotransmitter repletion by astrocytes that use TCA cycle intermediates to return carbon to the neurons (25,42). However, the agreement found between the rates determined for the glutamate/glutamine cycle measured by [1-^{13}C]glucose and the rates measured using glial-specific substrates (which take into account all cycling pathways) suggests that the glutamate/glutamine cycle is the major pathway under normal conditions in rodents and humans *in vivo* (5,20,21,25,41).

Controversies regarding the relationship between neuronal energetics and the glutamate/glutamine cycle

Despite the good agreement between findings by different investigators (see Fig. 3 and Table 1), there is considerable controversy regarding the relationship between the neuronal TCA cycle and V_{cyc}. The two major areas of debate are the proposed molecular mechanism and the slope of the relationship as a result of questions regarding the accuracy of measurement of V_{TCAn} and V_{cyc} (4,30,32,43). In the sections below, the controversies over the accuracy of determination of V_{TCAn} and V_{cyc} are discussed.

The fraction of glutamine synthesis as a result of anaplerosis via pyruvate carboxylase (PC) as opposed to neurotransmitter cycling

As shown in Fig. 1, in addition to neurotransmitter cycling, glutamine synthesis is used to replace glutamine that leaves the brain for ammonia detoxification and for the maintenance of nitrogen balance across the blood–brain barrier (5,17). Glutamine synthesis used to maintain nitrogen balance derives from anaplerosis via PC which, under normal conditions, appears to exclusively take place in astrocytes (and glial cells in general). The controversy regarding anaplerosis has largely been settled as a result of a convergence of results in animal models (5,11,19,20,23) and similar findings in the human brain (24,26) (see '*In vivo* ^{13}C MRS studies of human brain' section below). There is now general consensus that, in rat cerebral cortex, a minimum of 80% of glutamine synthesis supports neurotransmitter cycling under normal conditions and between 70 and 90% in humans. Of the remaining 20% of glutamine synthesized by anaplerosis, the majority is probably also used to replete neurotransmitter glutamate that is oxidized in glial cells (see below) as opposed to ammonia detoxification (5,26).

The effect of a slow rate of mitochondrial glutamate exchange (V_x) on the calculation of V_{TCAn}

Another factor that may influence the measured relationship is the rate of exchange of label from mitochondrial α-ketoglutarate to cytosolic glutamate, often termed 'V_x' in the literature. If this exchange is not much faster than the TCA cycle rate, it may cause an underestimation of V_{TCAn}, unless it is incorporated in metabolic modeling through measurement of the C2 and/or C3 positions of glutamate (24,44). Interestingly, it has been noted that, independent of whether multiple glutamate positions are measured, very little difference is found in the calculated values of V_{TCAn} or V_{cyc} in studies of human brain [see Hyder *et al*. (11)]. On the basis of numerical simulations, it has been shown that the accuracy of measurement of V_x in the brain using ^{13}C MRS is low (44,45), which most probably explains the extended controversy on this issue. Recently, Yang *et al*. (46), using an elegant saturation transfer method, have shown that V_x is, at minimum, several times greater than V_{TCAn} in the brain, explaining why it does not have an impact on measurements of V_{TCAn}.

In addition to the consistency of results between different studies and laboratories, V_{TCAn} values measured in rat and human cerebral cortex are consistent with results previously published using ^{14}C-2-deoxyglucose autoradiography, AV difference and PET (7,11). Recently, two studies have compared directly PET

Table 1. Experimental mean and standard deviation (SD) of V_{cyc}, V_{TCAn}, V_{TCAa}, V_{PC}, V_{cyc}/V_{Gln} and $V_{cyc}/0.5V_{TCAn}$ in the resting awake human midline occipital/parietal lobe from ^{13}C and ^{1}H–^{13}C MRS studies. As in the rat brain, the majority of human cortical glutamine synthesis is a result of the glutamate/glutamine cycle as shown by the average value of V_{cyc}/V_{Gln} of 0.83. Similarly, the ratio of $V_{cyc}/0.5V_{TCAn}$ of 0.75 is consistent with the coupling between V_{cyc} and V_{TCAn} measured in the rat cerebral cortex, and indicates that the majority of neuronal energy production in the resting awake human brain is likely to be devoted to the support of neuronal activity. Based on the relative values of V_{TCAa}, V_{TCAn} and $V_{PC,}$ approximately 20% of brain ATP production occurs in astrocytes

Reference	$V_{TCAtotal}$	V_{TCAn}	V_{TCAa}	V_{cyc}	V_{PC}	$V_{cyc}/0.5V_{TCAn}$	V_{cyc}/V_{Gln}
(45)[b]		0.73					
(58)		0.74		0.32	0.08	0.86	0.80
(27)	0.77	0.71	0.06	0.32	0.04	0.90	0.95
(57)[c]		0.66					
(84)[b]		0.83					
(75)	0.70		0.13				
(25)			0.12[a]	0.28[a]		0.78	
(148)		0.75		0.29			
(24)	0.63	0.57	0.06	0.17	0.09	0.60	0.65
(26)		0.72			0.02	0.73	0.93
(41)	0.65	0.53	0.13	0.16		0.64	
(140)			0.09				
(149)[b]		0.79					
Mean ± SD	0.69 ± 0.06	0.70 ± 0.09	0.09 ± 0.04	0.26 ± 0.08	0.06 ± 0.03	0.75 ± 0.12	0.83 ± 0.14

TCA, tricarboxylic acid; V_{cyc}, glutamate/glutamine cycle rate; V_{Gln}, glutamine synthesis rate; V_{PC}, rate of anaplerosis through pyruvate carboxylase; V_{TCAa}, astroglial TCA cycle rate; V_{TCAn}, neuronal TCA cycle rate; $V_{TCAtotal}$, sum of neuronal and astroglial TCA cycle rate.
[a]Measured steady state ratios converted to rates using the value of V_{TCAn} from Shen *et al.* (27).
[b]One-compartment model for the neuron used. We assume that the derived TCA rate most closely reflects V_{TCAn}.
[c]Average of white and gray matter rates which were measured separately.

measurements in nonhuman primates with ^{13}C MRS and found excellent agreement between the total rate of glucose metabolism measured (9,10).

Effects of isotopic dilution of glutamine on the calculated rate of neurotransmitter cycling (V_{cyc})

Shestov *et al.* (44) published the results of simulation studies in which they reported much poorer precision when measuring V_{cyc} using a [1-^{13}C]glucose precursor than reported in experimental papers. Shen *et al.* (47) were able to explain this discrepancy by showing that, when isotopic dilution of glutamine was taken into account, as had been performed in most previous experimental studies, but not in the simulations by Shestov *et al.* (44), the theoretical precision of the V_{cyc} measurement was similar to that reported experimentally. A similar conclusion regarding the importance of including glutamine dilution in metabolic modeling was arrived at by Oz *et al.* (20) when comparing rates calculated using [1-^{13}C]glucose and ^{14}C-CO_2 as precursors. We note that, when astrocyte-specific labels, such as [2-^{13}C]acetate, are used to determine V_{cyc}, alone or in combination with [1-^{13}C]glucose, considerably higher precision for the measurement of V_{cyc} is obtained (38,41).

Oxidation of the neurotransmitter glutamate

Glutamate released by neurons and taken up by astroglia can undergo oxidation as well as conversion to glutamine. The oxidized glutamate is then replaced by anaplerosis and cycled back to the neuron as glutamine (4). This scenario of oxidation and replacement by anaplerosis must occur in order to maintain constant levels of TCA cycle intermediates and glutamate-derived neurotransmitters, as the transport of the necessary five-carbon precursors from blood is comparatively minimal. This possibility is seen by several researchers as being in contradiction with the measured relationship between cycling and energetics (48). However, as described previously, the presence of glutamate oxidation has no impact on the MRS measurement of the glutamate/glutamine cycle using a glial-specific labeled precursor, such as [2-^{13}C]acetate, because the oxidized glutamate is replaced by *de novo* glutamine synthesis, which is cycled back to the neuron (5,25,26). When [1-^{13}C]glucose is used as the precursor, replacement of oxidized glutamate will be included in the anaplerotic contribution to glutamine synthesis, unless it is distinguished from glutamine synthesis related to ammonia removal (detoxification) on the basis of other measurements.

IN VIVO ^{13}C MRS STUDIES OF HUMAN BRAIN

In the sections below, we review the results from ^{13}C and ^{1}H–^{13}C MRS studies of human brain, focusing primarily on studies that report metabolic rates or labeling. Following initial studies of the animal brain in the 1980s (49–51), the availability of high-field human MR systems and improvements in $B_{\emptyset}$ shimming (52) led to the first ^{13}C and ^{1}H–^{13}C MRS studies of humans (16,53–55). Although the use of ^{13}C MRS in humans has been relatively limited (see 'Future prospects for ^{13}C MRS studies in humans' section below), ^{13}C MRS has already made major contributions to the understanding of human brain energetics and

neurotransmitter cycling and how alterations in these pathways may contribute to a range of human diseases.

^{13}C MRS measurements of the rate of the neuronal (V_{TCAn}) and astrocyte (V_{TCAa}) TCA cycle and V_{cyc} in human brain

Table 1 shows a compilation of studies from different groups measuring V_{TCAn}, V_{TCAa}, V_{PC} (rate of anaplerosis through pyruvate carboxylase) and V_{cyc} in the human midline occipital lobe. As can be seen, there is very good agreement in the rates derived by different studies, with most of the difference explainable by different volume fractions of white matter [which has an approximately three to four times lower rate of V_{TCAn} than gray matter (56,57)]. As discussed above, V_{TCAn} values are similar whether modeling uses the C4, C3 and C2 positions of glutamate and glutamine or just the C4 positions. For the measurement of V_{TCAa}, there is good agreement between three independent labeling strategies using [1-^{13}C]glucose, [2-^{13}C]acetate and ^{13}C-bicarbonate as precursors. In the human studies, V_{TCAn} largely reflects glutamatergic neurons, as it is derived from the fitting of the isotopic turnover of the large glutamate pool. Although the rate of the GABAergic neuron TCA cycle has not yet been determined, labeling of GABA during the infusion of [1-^{13}C]glucose has been reported at 4 T (24,58). Results in animal models suggest that on the order of 10% of the energy consumption of the cerebral cortex may be caused by GABAergic neurons (22,59).

Relationship between neuronal energetics and the glutamate/glutamine cycle in human brain and implications for resting brain functional activity

^{13}C MRS studies by several groups have found a ratio of V_{TCAn} to V_{cyc} that is highly consistent with the predictions based on studies performed in the rat. Table 1 shows the ratio of $V_{cyc}/0.5V_{TCAn}$ derived in human studies. The values range from 0.6 to 0.9 with an average of 0.75 ± 0.12. This average is similar to the value of $V_{cyc}/0.5V_{TCAn}$ predicted from animal studies using the best fit of the relationship between V_{cyc} and V_{TCAn} in Fig. 2. The variation in the ratio measured in humans is largely a result of variation in the measurement of V_{PC}. However, on the basis of AV measurements in humans, the majority of V_{PC} represents replacement of oxidized glutamate, and therefore reflects glutamine synthesis that is cycled back to the neuron (26). Overall, these studies show that functional neuronal activity is extremely high in the awake resting human brain and, if there is a similar relationship as in the rat, accounts for the majority of neuronal glucose consumption. Furthermore, the energy devoted to neuronal activity in the resting state is much higher than the changes in activity that occur during standard activation paradigms, such as cognitive challenges and visual stimulation (60). These findings have contributed to the recent surge in interest in the study of resting brain activity by functional MRI and other methods, and form part of the basis of several theories of resting brain function (60,61).

Measurements of the rate of glutamine synthesis via PC in human cerebral cortex

As a result of the astrocyte localization of PC, anaplerosis occurs only in the glia and is used both to synthesize glutamine that leaves the brain to maintain nitrogen balance and to replace released neurotransmitter glutamate oxidized in the astrocytes. In order to address the question of what fraction of glutamine synthesis occurs via the glutamate/glutamine cycle *versus* anaplerosis via PC, several studies in the human brain have measured this rate. As shown in Table 1, on the basis of these measurements, the fraction of glutamine synthesis via the glutamate/glutamine cycle (V_{cyc}/V_{Gln}, where V_{Gln} is the glutamine synthesis rate) has been reported to range between 0.65 and 0.93 in human cerebral cortex, with a mean value of 0.83 ± 0.14 (24,26,27). A complication when using the [1-^{13}C]glucose precursor to measure this ratio is that label enters the inner positions of glutamate via both pyruvate dehydrogenase and PC. To eliminate the complications arising from [1-^{13}C]glucose as precursor, Mason *et al*. (26) measured ^{13}C incorporation into glutamate and glutamine in the midline occipital/parietal lobe of human volunteers from infused [2-^{13}C] glucose, which labels the C2 and C3 positions of glutamine and glutamate primarily via PC. Labeling in glutamate C4 was used to assess the rate of pyruvate recycling coupled to glutamate oxidation. Metabolic modeling of the labeling data indicated that the PC flux (V_{PC}) ranges from 6 to 10% of the rate of glutamine synthesis (0.02–0.03 μmol/g/min). Comparison of the measurements of V_{PC} in humans to date with AV difference measurements of human brain glutamine efflux suggests that the majority of the PC flux is used to replace glutamate lost by oxidation in the glia and possibly elsewhere, and therefore can be considered to support neurotransmitter cycling (26).

Studies of substrate oxidation and transport

Because of its ability to distinguish a substrate from its metabolic products, ^{13}C MRS can be used to independently assess both the parameters of transport and rates of metabolism. Furthermore, it can be uniquely used to determine cell type-specific metabolism. Glucose has long been known to be the primary fuel for brain metabolism (28). However, the brain can also consume alternative substrates, including acetate, β-hydroxybutyrate and lactate. β-Hydroxybutyrate is a particularly important substrate during development and under conditions of fasting, where AV difference methods have revealed its capacity to supply up to 60% of the fuel oxidized by the brain (62). Similar high rates of utilization of lactate have been reported under conditions of elevated plasma lactate, such as during exercise (63,64). Although the total usage and oxidation of these substrates have been determined for humans by AV difference methods and, to some extent, by PET, the ^{13}C MRS studies reviewed below have provided the first information on the cell type specificity of substrate usage, as well as revealing new insights into the blood–brain transport of these substrates.

Glucose

As a result of the commercial availability of [1-^{13}C]glucose and the high rate of brain glucose metabolism, the majority of metabolic ^{13}C MRS studies have focused on the measurement of neuronal and glial glucose metabolism [see '^{13}C MRS measurements of the rate of the neuronal (V_{TCAn}) and astrocyte (V_{TCAa}) TCA cycle and V_{cyc} in human brain' section above]. ^{13}C MRS has been used to measure glucose transport parameters (apparent Michaelis–Menten constant of transport and maximal unidirectional transport rate) in the human midline occipital/parietal lobe (54). Subsequent studies of brain glucose transport in humans have used ^{1}H MRS for higher sensitivity. These studies have provided support for the blood–brain barrier being the rate-limiting step for

human brain glucose transport (65), which is best described by a reversible, Michaelis–Menten transport model [as opposed to the nonreversible model used previously to interpret most PET glucose studies (66,67)] (68,69). In this model, glucose transport is described by transporters with reversible Michaelis–Menten kinetics across the membranes of the capillary endothelial cells that make up the blood–brain barrier (66,67). On the basis of *in vivo* kinetic and isolated transporter studies, the glial and neuronal glucose transporters have a relatively much higher activity and can, to a first order, be neglected in the kinetic modeling. These results have been used to develop and test kinetic models of glucose transport and metabolism (68), and may have potential value for the assessment of whether impaired substrate delivery may have an impact on brain function in disease (70).

Acetate

Studies in animal models and neural cell culture have found that acetate is almost exclusively transported into and metabolized by the astroglia (37,71–74). Lebon *et al*. (25) studied healthy human subjects infused intravenously with [2-^{13}C]acetate whilst monitoring ^{13}C labeling in the midline occipital/parietal lobe with ^{13}C MRS. The concentration of brain acetate was approximately 10-fold lower than the plasma concentration, indicating that acetate transport was primarily unidirectional. Analysis of the steady-state ^{13}C labeling pattern of glutamine and glutamate, as shown in Fig. 2, as well as the kinetics of glutamate and glutamine labeling was consistent with acetate metabolism localized to glial cells (25). Furthermore, the steady-state labeling patterns were in agreement with findings from [1-^{13}C]glucose of a high rate of glutamate/glutamine cycling (25,41). Similar conclusions were obtained by Blüml *et al*. (75) using [1-^{13}C]acetate as a precursor. Although normal plasma levels of acetate in humans are relatively low, the levels can be elevated to approximately 1 mM or more by alcohol consumption, becoming a major source of oxidative energy for the astrocyte (25,41,75,76).

β-Hydroxybutyrate

β-Hydroxybutyrate is a substrate critical for brain function during fasting. β-Hydroxybutyrate enters the brain via facilitated diffusion using a monocarboxylate carrier at the blood–brain barrier (70). Although brain β-hydroxybutyrate consumption had been studied extensively using AV difference methods, it was not known whether β-hydroxybutyrate was preferentially consumed in neurons or astrocytes, or whether the blood–brain barrier was limiting for its metabolism (28). To answer these questions, localized ^{13}C MRS measurements were performed during an infusion of [2,4-^{13}C]β-hydroxybutyrate in healthy subjects, and the entry and metabolism of this compound were measured in the medial occipital/parietal cortex (77). During the 2-h infusion study, ^{13}C label was detected in the β-hydroxybutyrate resonance positions at a time resolution of 5 min and in the amino acid pools of glutamate, glutamine and aspartate. The pattern of ^{13}C labeling at the steady-state period (60–120 min) was very different from that resulting from infusions of ^{13}C-acetate, but was broadly similar to that of [1-^{13}C]glucose, indicating a predominant neuronal consumption of this substrate. The cortical β-hydroxybutyrate concentration (0.18 mM) was much lower than in plasma (2 mM), indicating that transport across the blood–brain barrier limits brain β-hydroxybutyrate metabolism. The consumption of β-hydroxybutyrate accounted for approximately 6% of total brain oxidative metabolism in nonfasted volunteers, consistent with earlier reports using AV difference methods (28).

Lactate

Studies over the last decade have provided evidence that lactate may be an important metabolic fuel for the brain, including proposals that an astrocyte-to-neuron lactate shuttle may exist in order to provide neurons with fuel during periods of enhanced activity (30,32). In addition, AV difference and PET studies of humans after blood lactate elevation by exercise have reported that elevated lactate can provide a significant fraction of oxidative fuel to the brain (63,64). To determine the conditions under which plasma lactate might contribute as a significant fuel for human brain energy metabolism, Boumezbeur *et al*. (78) infused [3-^{13}C]lactate and measured, by ^{13}C MRS, the entry and utilization of lactate in the midline occipital/parietal cortex of healthy human volunteers. During the 2-h infusion study, ^{13}C incorporation in the amino acid pools of glutamate and glutamine was measured every 5 min. With a plasma concentration of lactate in the 0.8–2.8 mmol/L range, the brain tissue lactate concentration was assessed, as was the fractional contribution of lactate to brain energy metabolism. By fitting the measured relationship between the unidirectional lactate influx and the plasma and brain lactate concentrations, the lactate transport constants were calculated using a model in which the rate-limiting step was assumed to be, on the basis of previous work, lactate transport at the blood–brain barrier. The transporters at the blood–brain barrier were modeled as reversible Michaelis–Menten transporters, similar to that performed with glucose transport. The results showed that, in the physiological range of plasma lactate concentration, the unidirectional rate of transport and concentration of brain lactate increased linearly with plasma concentration. The maximum potential contribution of plasma lactate to brain metabolism was 10% for a basal plasma lactate concentration of approximately 1.0 mM, and possibly as much as 60% at supraphysiological plasma lactate concentrations when the transporters are saturated (assuming that lactate oxidation is limited only by transport). Based on the similarity of the steady-state pattern of ^{13}C labeling, as shown in Fig. 2, it was concluded that the relative consumption of plasma lactate between neurons and astrocytes is similar to that of glucose (78). The calculation of the lactate metabolic capacity is in good agreement with recent AV difference studies using isotopically labeled lactate as a tracer, further confirming the potential importance of plasma lactate as a substrate for brain metabolism (63).

Use of ^{1}H–^{13}C MRS to study the energetics of brain tissue types (white/gray matter) and sensory stimulation

As described in the 'Future prospects for ^{13}C MRS studies in humans' section below, the sensitivity and spatial resolution limitations of ^{13}C MRS can be partially overcome by using the more sensitive ^{1}H nucleus to measure the ^{13}C enrichment of bound carbon atoms. These inverse MRS methods take advantage of the *J* coupling between ^{1}H and ^{13}C nuclei (51,79). By combining ^{1}H–^{13}C MRS with spectroscopic imaging and gray/white matter segmentation, Pan *et al*. (57) reported V_{TCAn} in gray and white matter, finding an approximately four times higher rate of metabolism in gray matter. The higher resolution of ^{1}H–^{13}C MRS has been used to address the question of whether glycolytic or oxidative ATP production provides most of the incremental

energy for brain function during activation (11,80–83). Using this technique, Chen *et al*. (84) reported a 25% increase in V_{TCAn} during visual stimulation. This finding is consistent with recent calibrated functional MRI measurements of the cerebral metabolic rate of oxygen consumption (85–87), and indicates that ATP produced oxidatively is the major source of energy for the incremental neuronal activity during sensory stimulation.

Application of ^{13}C MRS to study neuroenergetics and neurotransmission in human brain disease

The important role of neuroenergetics and the glutamate/GABA neurotransmitter cycles in the pathogenesis of brain disease is being increasingly recognized. Changes in the concentrations of GABA, glutamate and glutamine have been measured by ^{1}H MRS in a wide range of neurological and psychiatric diseases, including aging (88), depression and related disorders (89–94), epilepsy (95–97), genetic disorders of metabolism (98), hepatic encephalopathy (99) and neurodegenerative disorders (100). However, concentration measurements, although informative, are not specific for the alterations in metabolic fluxes or cellular neurochemical distributions that may have led to these changes. ^{13}C MRS allows the measurement of metabolic rates in humans, and may potentially be of great value in studying the pathogenesis and treatment of brain disease. However, its application to disease has been limited by several factors, including the technical complexity of conducting ^{13}C MRS experiments, which is exacerbated by the lack of study support with most clinical scanners. Furthermore, there is the need for a support team to perform the infusion and analysis of substrates labeled with the ^{13}C isotope. Moreover, further problems include the relatively low sensitivity and volume resolution of ^{13}C MRS compared with ^{1}H MRS (and especially MRI), the availability and cost of ^{13}C-labeled substrates, radiofrequency (RF) heating concerns with the need to decouple the *J* interaction of ^{13}C resonances with bound protons, and the need to perform sophisticated kinetic analysis to extract metabolic rate information from the MRS data [see Ross *et al*. (101) for an informative review on clinical ^{13}C MRS studies in humans and the obstacles in performing them]. In the 'Future prospects for ^{13}C MRS studies in humans' section below, we speculate on how some of these barriers may be overcome through a range of developments, including hyperpolarized ^{13}C. Despite these challenges, the initial applications of ^{13}C MRS in studies of human brain disease and dysfunction have been highly informative, and are reviewed briefly below.

Application of ^{13}C MRS to study stroke and tumors

The initial application of ^{13}C MRS to clinical brain disease was to assess the source of chronic lactate elevation in stroke. In this study, ^{1}H MRS was used to measure lactate ^{13}C fractional enrichment in an infarct during the infusion of [1-^{13}C]glucose. ^{1}H MRS was used because of its several-fold higher sensitivity for the measurement of ^{13}C enrichment than direct ^{13}C MRS (102). Lactate was found to rapidly incorporate label from glucose, indicating active metabolic production long after the initial infarct event (103). Subsequent ^{1}H MRS and histological assessment indicated that most of the lactate elevation in chronic stroke was probably a result of macrophage metabolic activity and infiltration (104). A similar strategy was used in animal models of brain cancer by Terpstra *et al*. (105) to assess the metabolic source of lactate in tumors. Recently, ^{13}C MRS has been used to measure lactate turnover in a human brain tumor (106).

Application of ^{13}C MRS to study hepatic encephalopathy and genetic diseases of ammonia metabolism

Studies by Ross and coworkers (23,99) and other laboratories (107,108) have established ^{1}H MRS measurements of glutamine and glutamate as one of the best ways to assess the severity of hepatic encephalopathy, a disease of the brain caused by chronic exposure to elevated ammonia in the blood as a result of liver failure. Animal studies using conventional methods, as well as ^{13}C and ^{15}N MRS, showed that ammonia led to increased anaplerosis and glutamine synthesis in astrocytes, as well as to disruption of the glutamate/glutamine cycle (5,17,27,109–112). To test whether similar metabolic alterations were present in humans, Blüml *et al*. (113) studied patients with diagnosed hepatic encephalopathy during the infusion of [1-^{13}C]glucose at 1.5 T. The studies found disrupted neuroenergetics with increasing disease severity, including evidence of impairment of the glutamate/glutamine cycle. More recently, Gropman *et al*. (114) have used ^{13}C MRS to demonstrate abnormalities in glutamate metabolism in patients with ornithine transcarbamylase deficiency.

Application of ^{13}C MRS to study Alzheimer's disease and healthy aging

Mitochondrial dysfunction has been implicated in the loss of brain function in neurodegenerative disease and normal aging (115). Studies using PET have found decreased rates of brain oxygen consumption and glucose consumption in Alzheimer's disease and in healthy aging (116,117). In a pioneering study on Alzheimer's disease, Lin *et al*. (118) infused two patients with [1-^{13}C]glucose and found a reduction in ^{13}C labeling of C4 glutamate, consistent with an impairment in the TCA cycle. Recently, Boumezbeur *et al*. (41), using combined infusions of [1-^{13}C]glucose and [2-^{13}C]acetate with ^{13}C MRS, compared a healthy group of elderly subjects with young adult controls. The elderly subjects showed decreased V_{TCAn} and V_{cyc}, together with increased V_{TCAa}, changes which were independent of the relatively small age-dependent loss of brain tissue volume. The decrease in V_{TCAn} correlated highly with decreases in *N*-acetylaspartate and glutamate concentrations (Fig. 4), indicating that the reduced metabolic rates were associated with cellular level changes as opposed to differences in sensory input. These findings are consistent with the theory that mitochondria lose oxidative capacity with advancing age, leading to a loss of brain function. Overall, the ability to study aging and associated dementias with ^{13}C MRS provides a unique opportunity to study the role of mitochondria in the pathogenesis process and how this process can be slowed or ceased through treatment.

Application of ^{13}C MRS to study the complications of type 1 diabetes

A major complication in insulin therapy for type 1 diabetes is hypoglycemia, the frequency of which is worsened by the phenomenon of hypoglycemia unawareness (119,120). Among the theories to explain this phenomenon is that repeated hypoglycemic episodes in patients with type 1 diabetes may lead to metabolic adaptations that allow improved function during periods of mild hypoglycemia. Using [2-^{13}C]acetate as a tracer, Mason *et al*. (76) tested the hypothesis that patients with type 1 diabetes

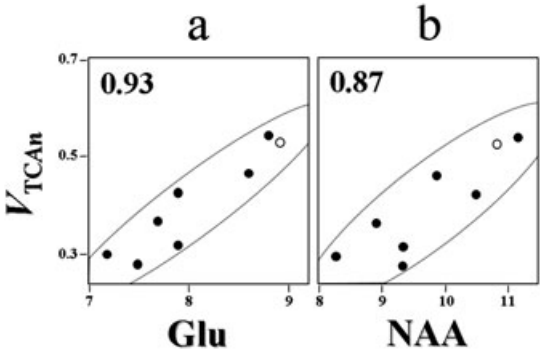

Figure 4. Comparison of V_{TCAn} *versus* glutamate (Glu) and *N*-acetylaspartate (NAA) concentration in the midline occipital/parietal lobe of healthy elderly subjects. The results show a strong correlation between the rate of the neuronal tricarboxylic acid (TCA) cycle and the concentrations Glu and NAA, both of which have been associated with cellular dysfunction and chronically reduced mitochondrial activity in other studies. Pearson correlation coefficients are shown in the top left-hand corners of (a) and (b). Filled circles, values measured for the individual elderly subjects ($n = 7$); open circles, average values for the respective metabolite concentrations from a young cohort ($n = 7$). Fluxes and metabolite concentrations are expressed as μmol/g/min and μmol/g, respectively.

have upregulated blood–brain transport and metabolism of monocarboxylic acids (e.g., acetate, β-hydroxybutyrate and lactate), supporting heightened brain function during hypoglycemia. In their study of the medial occipital/parietal cortex, patients with type 1 diabetes showed increased metabolism of acetate, which was most probably secondary to increased acetate transport. An example of the higher ^{13}C labeling attained in patients with type 1 diabetes is shown in Fig. 5. A blood concentration of 1 mM acetate was found to provide, on average, approximately20% of astrocyte oxidative needs in control subjects and approximately 35% in patients with type 1 diabetes. Oz *et al*. (121) used ^{13}C MRS to show that brain glycogen may be a significant fuel source during hypoglycemia, and that hypoglycemia leads to elevated glycogen synthesis on restoration of normal glucose levels. Future studies may be able to determine whether these alternative fuel sources can account fully for the cortical component of hypoglycemia unawareness.

Application of ^{13}C MRS to study epilepsy

Epilepsy has been studied extensively by ^{1}H MRS and there is considerable evidence from PET, ^{1}H MRS and ^{31}P MRS of hypometabolism in brain regions affected by epilepsy that may be secondary to a failure in neuroenergetics (122). Furthermore, in medial temporal lobe epilepsy, chronically elevated extracellular glutamate has been found by microdialysis in epileptogenic sclerotic tissue, possibly contributing to the hyperexcited state of the tissue (123). In order to test whether the chronically elevated extracellular glutamate was a result of an impairment in glial glutamate uptake and cycling, Petroff *et al*. (124) obtained neurosurgical specimens from patients infused intravenously with [2-^{13}C] glucose, and analyzed the labeling *ex vivo* using high-resolution ^{13}C MRS. In the epileptogenic tissue from the hippocampus with sclerosis and glial proliferation, there was marked impairment in glutamate/glutamine cycling compared with more histologically normal tissue (124). A subsequent study showed that this impairment in glutamate/glutamine cycling may be secondary to reduced activity in glutamine synthetase, establishing this step in the pathophysiology and as a potential therapeutic target (125).

Application of ^{13}C MRS to study pediatric disease

The increasing concerns over radiation dosages in PET scans of pediatric patients have provided additional motivation for the noninvasive application of ^{13}C MRS in this vulnerable group. Studies of infants and young children with ^{13}C MRS, however, are complicated by the need for extended infusion times, increasing the time spent in the magnet. To assess the feasibility of pediatric studies, Blüml *et al*. (126) performed ^{13}C MRS on 17 children and pediatric patients receiving [1-^{13}C]glucose either

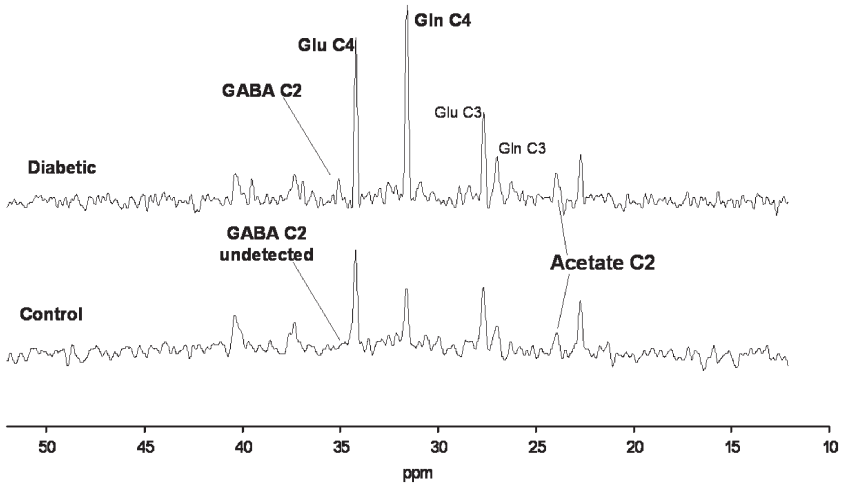

Figure 5. Comparison of steady-state ^{13}C MRS spectra during [2-^{13}C]acetate infusion of a patient with type 1 diabetes and a healthy control subject. Brain ^{13}C MRS spectra were averaged over the final 45 min of a hypoglycemic period during infusion of [2-^{13}C]acetate. The patient with diabetes (top spectrum) showed significantly greater labeling in glutamate (Glu) and glutamine (Gln) C4 than the control (bottom spectrum). The acetate C2 signal was also greater in the patient with diabetes. Other resonances labeled in the figure include γ-aminobutyric acid (GABA) C2 and Glu C3.

orally or intravenously. They observed marked differences in ^{13}C labeling patterns in premature brain and pediatric patients with leukodystrophies and mitochondrial disorders. This study demonstrates the significant potential of ^{13}C MRS applications to pediatric disease, particularly with the improvements in sensitivity discussed below.

FUTURE PROSPECTS FOR ^{13}C MRS STUDIES IN HUMANS

As discussed above, there are several major challenges that must be met for ^{13}C MRS to become a routine tool in the study of human brain disease and treatment. Below, we briefly discuss these limitations, and how they may be overcome through future technological developments.

Improvements in the sensitivity and spatial resolution of ^{13}C MRS measurements

The primary limitation for the study of human brain disease by ^{13}C MRS is its low sensitivity, with the typical volume resolution being on the order of 25–100 cm^3. Substantial improvements have been achieved by detecting ^{13}C labeling indirectly via the *J* scalar coupling to bound protons (55,103), enhancing the spatial resolution to several cubic centimeters obtained at 4 T (57,84). However, because of the limited spectral resolution of ^{1}H MRS, only labeling of glutamate C4, the combined resonances of glutamate and glutamine C3, and lactate C3 have been reported, limiting the rates that can be measured to the neuronal TCA cycle or, in the case of elevated lactate, to glycolysis. With the advent of ultrahigh-field human MRS systems (7 T and above), in principle, it should be possible to measure resonances of glutamine and GABA, as has been demonstrated in animal studies (59,127,128), although the increased heating associated with decoupling at higher fields may limit this application.

An alternative possibility, which would retain the high spectral resolution and information of direct ^{13}C MRS, and provide much higher spatial resolution, is the use of hyperpolarized ^{13}C MRS, and there have been several promising initial reports in animal models (129–131). The major limitations in the measurement of the rates of the pathways discussed in this article are that there are several enzymatic steps between the precursor (e.g. acetate, lactate, glucose) and enzymatic reactions in the pathways of interest. For example, to measure V_{cyc} from hyperpolarized ^{13}C-acetate, the acetate must first be transported into glial cells and then converted successively to acetyl-CoA, citrate, isocitrate, α-ketoglutarate and glutamate, before being converted by glutamine synthetase into glutamine. Based on the concentration of the precursor pools and the metabolic rate of acetate metabolism, it would take on the order of 1–2 min for the immediate precursor glial glutamate to be labeled sufficiently to measure the glutamine synthesis rate. Measurement of the glial and neuronal TCA cycle, and anaplerosis, may be feasible by the direct examination of TCA cycle intermediates (e.g. citrate) from precursors such as [2-^{13}C]acetate and [2-^{13}C]lactate, which label TCA cycle intermediates in one or two enzymatic steps. An alternative approach is to hyperpolarize directly TCA cycle intermediates themselves, the feasibility of which has been demonstrated in extracts (131).

Improvements in shimming and reduction in RF heating to allow multi-volume ^{13}C MRS

To date, the majority of human brain ^{13}C MRS studies have been performed in the midline occipital or occipital/parietal lobe, largely because of the relative ease of shimming to improve $B_{\varnothing}$ homogeneity in this region and the distance from the eyes, which are believed to be more sensitive than the brain to heating from the decoupling B_1 field. Over the last decade, limitations of shimming have been greatly reduced as a result of improvements in shim coil strengths and advanced field mapping and shim calculation and updating methods, allowing well-shimmed spectra to be obtained from multiple volumes within the human brain even at ultrahigh fields (52,132–134).

A continuing limitation is the heating that results from the applied RF energy to the protons bound to ^{13}C needed to decouple the *J* interaction. It has been shown that there are theoretical limits on the minimum decoupling power (135) which, even at 4 T, are close to the allowable power deposition limits mandated by the US Food and Drug Administration (136). Although advances in RF coil design have allowed human brain ^{13}C studies to be performed safely even up to 4 T (137,138), concerns remain about RF heating of the eyes, which may be more vulnerable than the brain because of areas of restricted circulation. A recently developed alternative approach to circumvent RF heating is to observe ^{13}C labeling of the carboxyl groups of glutamate and glutamine which require no (or low-power) decoupling (139,140). This approach takes advantage of the turnover kinetics of glutamate C5 from exogenous [2-^{13}C]glucose, which is

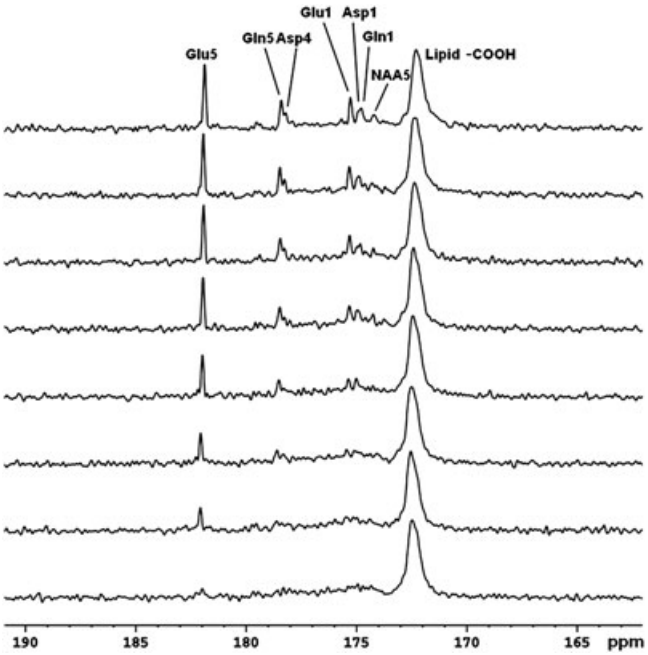

Figure 6. ^{13}C MRS time course spectra of glutamate (Glu), glutamine (Gln) and aspartate (Asp) turnover detected in the occipital lobe during the intravenous infusion of [2-^{13}C]glucose. Lorentzian–Gaussian transformation (Lorentzian broadening (LB) = 3 Hz, Gaussian broadening (GB) = −0.3) was applied. The time-averaged decoupling power was 1.46 W. Each spectrum corresponds to 8.5 min of signal averaging (128 scans). Glu C5 (182.0 ppm) and C1 (175.4 ppm), Gln C5 (178.5 ppm) and C1 (174.9 ppm), Asp C4 (178.3 ppm) and C1 (175.0 ppm) and *N*-acetylaspartate (NAA) C5 (174.3 ppm) were detected. No baseline corrections were made. Figure adapted from Li *et al.* (141).

identical to the turnover of glutamate C4 from exogenous [1-^{13}C]glucose (141). The carboxylic carbons are only coupled to protons via very weak long-range ^{1}H–^{13}C scalar couplings, so that they can be effectively decoupled at low RF power. An additional advantage of this strategy is the lack of contamination from subcutaneous lipids, because there are no overlapping fat signals in the vicinity of the glutamate C5 and glutamine C5 peaks. An example showing the feasibility of this strategy at 3 T is the work of Li *et al*. (141) (Fig. 6). High-quality spectra can be obtained with a maximum regional power deposition in the brain below 2 W/kg, several times below the US Food and Drug Administration limit, even using a ^{1}H resonator to deliver the RF decoupling field (142). The ability to deliver RF decoupling from a volume coil further opens up the possibility of multi-volume whole-brain ^{13}C MRS.

An alternative approach to reduce RF heating would be to use hyperpolarized ^{13}C MRS without decoupling. The higher sensitivity of hyperpolarized ^{13}C would, in principle, make decoupling unnecessary. However, as a result of the blood–brain barrier restricting the ability to isotopically label brain metabolites from plasma, ^{13}C-labeled substrate decoupling may be necessary even for hyperpolarized ^{13}C MRS applications.

Improvements in ^{13}C infusion protocols

A third major limitation in ^{13}C MRS studies is the requirement for a continuous infusion of the isotopically labeled substrate with venous sampling for fractional enrichment determination. This infusion must occur over a time period (typically 2 h) to capture sufficient kinetic information from spectral time courses for absolute rate estimation using metabolic modeling (24,45,143). However, several studies have shown that it is possible to obtain considerable information on metabolism using simplified infusion schemes or oral ingestion (144–147). Given that the majority of information on absolute and relative rates is derived from the early and steady-state portions of the time course, a significant reduction in the time required for a subject to be in the scanner may be possible (143).

CONCLUSIONS

Work over the past two decades has established ^{13}C MRS studies of the brain in animal models and humans as the only noninvasive method for the measurement of neuronal and glial energy metabolism and glutamate and GABA neurotransmitter cycling. Although some debate regarding metabolic modeling remains, much of our present knowledge of the brain energy budget (glutamatergic neurons, GABAergic neurons, astrocytes) and the relationship between neuroenergetics and neurotransmission has been obtained from *in vivo* ^{13}C MRS studies. ^{13}C MRS studies have also played an important role in delineating how alternative substrates, such as acetate, ketone bodies and lactate, support neuronal and astrocyte energetics. The application of ^{13}C MRS to the study of human disease faces considerable obstacles, particularly the cost, the need for ^{13}C substrate infusions and monitoring, decoupling heating and the low sensitivity of ^{13}C MRS and lack of technical capability of most MR systems. Despite these difficulties, ^{13}C MRS has been successfully applied to the study of a variety of neurological and psychiatric diseases, as well as diabetes and healthy aging. The increasing availability of high-field MR magnets, which allow higher sensitivity indirect detection methods, and the development of hyperpolarized ^{13}C have the potential to greatly increase the sensitivity of the method, leading to the possibility of using ^{13}C MRS for metabolic imaging of the human brain. These technological developments, together with further improvements in ^{13}C infusion protocols to minimize patient time in the magnet, have the potential to greatly expedite clinical and research studies.

Acknowledgements

This work was supported by grants R01-DK027121, P30-NS052519, R01-EB000473, R01-MH95104, R01-DA021785 R21-AA018210, R21-AA019803 from NIH and 10A087 from AICR. We thank Dr Jun Shen for providing the figure 6.

REFERENCES

1. Shephard GM. *The Synaptic Organization of the Brain*. Oxford University Press, Oxford; 1994.
2. Rothstein JD, Dykes-Hoberg M, Pardo CA, Bristol LA, Jin L, Kuncl RW, Kanai Y, Hediger MA, Wang Y, Schielke JP, Welty DF. Knockout of glutamate transporters reveals a major role for astroglial transport in excitotoxicity and clearance of glutamate. Neuron, 1996; 16(3): 675–686.
3. Bergles DE, Diamond JS, Jahr CE. Clearance of glutamate inside the synapse and beyond. Curr. Opin. Neurobiol. 1999; 9(3): 293–298.
4. Hertz L, Peng L, Dienel GA. Energy metabolism in astrocytes: high rate of oxidative metabolism and spatiotemporal dependence on glycolysis/glycogenolysis. J. Cereb. Blood Flow Metab. 2007; 27(2): 219–249.
5. Sibson NR, Mason GF, Shen J, Cline GW, Herskovits AZ, Wall JE, Behar KL, Rothman DL, Shulman RG. In vivo (13)C NMR measurement of neurotransmitter glutamate cycling, anaplerosis and TCA cycle flux in rat brain during [2-^{13}C] glucose infusion. J. Neurochem. 2001; 76(4): 975–989.
6. Yu AC, Drejer J, Hertz L, Schousboe A. Pyruvate carboxylase activity in primary cultures of astrocytes and neurons. J. Neurochem. 1983; 41(5): 1484–1487.
7. Rothman DL, Behar KL, Hyder F, Shulman RG. In vivo NMR studies of the glutamate neurotransmitter flux and neuroenergetics: implications for brain function. Annu. Rev. Physiol. 2003; 65: 401–427.
8. Mason GF, Rothman DL. Graded image segmentation of brain tissue in the presence of inhomogeneous radio frequency fields. Magn. Reson. Imaging, 2002; 20(5): 431–436.
9. Boumezbeur F, Besret L, Valette J, Gregoire M-C, Delzescaux T, Maroy R, Vaufrey F, Gervais P, Hantraye P, Bloch G, Lebon V. Glycolysis versus TCA cycle in the primate brain as measured by combining ^{18}F-FDG PET and ^{13}C-NMR. J. Cereb. Blood Flow Metab. 2005; 25 (11): 1418–1423.
10. Chaumeil MM, Valette J, Guillermier M, Brouillet E, Boumezbeur F, Herard A-S, Bloch G, Hantraye P, Lebon V. Multimodal neuroimaging provides a highly consistent picture of energy metabolism, validating ^{31}P MRS for measuring brain ATP synthesis. Proc. Natl. Acad. Sci. USA, 2009; 106(10): 3988–3993.
11. Hyder F, Patel AB, Gjedde A, Rothman DL, Behar KL, Shulman RG. Neuronal–glial glucose oxidation and glutamatergic–GABAergic function. J. Cereb. Blood Flow Metab. 2006; 26(7): 865–877.
12. Van den Berg CJ, Krzalić L, Mela P, Waelsch H. Compartmentation of glutamate metabolism in brain. Evidence for the existence of two different tricarboxylic acid cycles in brain. Biochem. J. 1969; 113(2): 281–290.
13. Hertz L. Functional interactions between neurons and astrocytes I. Turnover and metabolism of putative amino acid transmitters. Prog. Neurobiol. 1979; 13(3): 277–323.
14. Maycox PR, Hell JW, Jahn R. Amino acid neurotransmission: spotlight on synaptic vesicles. Trends Neurosci. 1990; 13(3): 83–87.
15. Nicholls D, Attwell D. The release and uptake of excitatory amino acids. Trends Pharmacol. Sci. 1990; 11(11): 462–468.
16. Gruetter R, Novotny EJ, Boulware SD, Mason GF, Rothman DL, Shulman GI, Prichard JW, Shulman RG. Localized ^{13}C NMR spectroscopy in the human brain of amino acid labeling from D-[1-^{13}C]glucose. J. Neurochem. 1994; 63(4): 1377–1385.
17. Cooper AJ, Plum F. Biochemistry and physiology of brain ammonia. Physiol. Rev. 1987; 67(2): 440–519.

18. Sibson NR, Dhankhar A, Mason GF, Behar KL, Rothman DL, Shulman RG. In vivo ^{13}C NMR measurements of cerebral glutamine synthesis as evidence for glutamate–glutamine cycling. Proc. Natl. Acad. Sci. USA, 1997; 94(6): 2699–2704.
19. Lieth E, LaNoue KF, Berkich DA, Xu B, Ratz M, Taylor C, Hutson SM. Nitrogen shuttling between neurons and glial cells during glutamate synthesis. J. Neurochem. 2001; 76(6): 1712–1723.
20. Oz G, Berkich DA, Henry P-G, Xu Y, LaNoue K, Hutson SM, Gruetter R. Neuroglial metabolism in the awake rat brain: CO2 fixation increases with brain activity. J. Neurosci. 2004; 24(50): 11 273–11 279.
21. Shen J, Sibson NR, Cline G, Behar KL, Rothman DL, Shulman RG. ^{15}N-NMR spectroscopy studies of ammonia transport and glutamine synthesis in the hyperammonemic rat brain. Dev. Neurosci. 1998; 20(4–5): 434–443.
22. Patel AB, de Graaf RA, Mason GF, Rothman DL, Shulman RG, Behar KL. The contribution of GABA to glutamate/glutamine cycling and energy metabolism in the rat cortex in vivo. Proc. Natl. Acad. Sci. USA, 2005; 102(15): 5588–5593.
23. Kanamori K, Kondrat RW, Ross BD. ^{13}C enrichment of extracellular neurotransmitter glutamate in rat brain – combined mass spectrometry and NMR studies of neurotransmitter turnover and uptake into glia in vivo. Cell Mol. Biol. (Noisy-le-grand), 2003; 49(5): 819–836.
24. Gruetter R, Seaquist ER, Ugurbil K. A mathematical model of compartmentalized neurotransmitter metabolism in the human brain. Am. J. Physiol. Endocrinol. Metab. 2001; 281(1): E100–E112.
25. Lebon V, Petersen KF, Cline GW, Shen J, Mason GF, Dufour S, Behar KL, Shulman GI, Rothman DL. Astroglial contribution to brain energy metabolism in humans revealed by ^{13}C nuclear magnetic resonance spectroscopy: elucidation of the dominant pathway for neurotransmitter glutamate repletion and measurement of astrocytic oxidative metabolism. J. Neurosci. 2002; 22(5): 1523–1531.
26. Mason GF, Petersen KF, de Graaf RA, Shulman GI, Rothman DL. Measurements of the anaplerotic rate in the human cerebral cortex using ^{13}C magnetic resonance spectroscopy and [1-^{13}C] and [2-^{13}C] glucose. J. Neurochem. 2007; 100(1): 73–86.
27. Shen J, Petersen KF, Behar KL, Brown P, Nixon TW, Mason GF, Petroff OA, Shulman GI, Shulman RG, Rothman DL. Determination of the rate of the glutamate/glutamine cycle in the human brain by in vivo ^{13}C NMR. Proc. Natl. Acad. Sci. USA, 1999; 96(14): 8235–8240.
28. Siesjo BK. *Brain Energy Metabolism*. Wiley, Chichester, New York; 1978.
29. Sibson NR, Dhankhar A, Mason GF, Rothman DL, Behar KL, Shulman RG. Stoichiometric coupling of brain glucose metabolism and glutamatergic neuronal activity. Proc. Natl. Acad. Sci. USA, 1998; 95(1): 316–321.
30. Magistretti PJ, Pellerin L, Rothman DL, Shulman RG. Energy on demand. Science, 1999; 283(5401): 496–497.
31. Shulman RG, Hyder F, Rothman DL. Cerebral energetics and the glycogen shunt: neurochemical basis of functional imaging. Proc. Natl. Acad. Sci. USA, 2001; 98(11): 6417–6422.
32. Jolivet R, Magistretti PJ, Weber B. Deciphering neuron–glia compartmentalization in cortical energy metabolism. Front Neuroenergetics, 2009; 1: 4.
33. Occhipinti R, Somersalo E, Calvetti D. Astrocytes as the glucose shunt for glutamatergic neurons at high activity: an in silico study. J. Neurophysiol. 2009; 101(5): 2528–2538.
34. Strelnikov K. Neuroimaging and neuroenergetics: brain activations as information-driven reorganization of energy flows. Brain Cogn. 2010; 72(3): 449–456.
35. Attwell D, Laughlin SB. An energy budget for signaling in the grey matter of the brain. J. Cereb. Blood Flow Metab. 2001; 21(10): 1133–1145.
36. Chowdhury GMI, Patel AB, Mason GF, Rothman DL, Behar KL. Glutamatergic and GABAergic neurotransmitter cycling and energy metabolism in rat cerebral cortex during postnatal development. J. Cereb. Blood Flow Metab. 2007; 27(12): 1895–1907.
37. Hassel B, Bachelard H, Jones P, Fonnum F, Sonnewald U. Trafficking of amino acids between neurons and glia in vivo. Effects of inhibition of glial metabolism by fluoroacetate. J. Cereb. Blood Flow Metab. 1997; 17(11): 1230–1238.
38. Patel AB, Chowdhury GMI, de Graaf RA, Rothman DL, Shulman RG, Behar KL. Cerebral pyruvate carboxylase flux is unaltered during bicuculline-seizures. J. Neurosci. Res. 2005; 79(1–2): 128–138.
39. Serres S, Raffard G, Franconi J-M, Merle M. Close coupling between astrocytic and neuronal metabolisms to fulfill anaplerotic and energy needs in the rat brain. J. Cereb. Blood Flow Metab. 2008; 28(4): 712–724.
40. Patel AB, de Graaf RA, Rothman DL, Behar KL, Mason GF. Evaluation of cerebral acetate transport and metabolic rates in the rat brain in vivo using ^{1}H–[^{13}C]-NMR. J. Cereb. Blood Flow Metab. 2010; 30(6): 1200–1213.
41. Boumezbeur F, Mason GF, de Graaf RA, Behar KL, Cline GW, Shulman GI, Rothman DL, Petersen KF. Altered brain mitochondrial metabolism in healthy aging as assessed by in vivo magnetic resonance spectroscopy. J. Cereb. Blood Flow Metab. 2010; 30(1): 211–221.
42. Maciejewski PK, Rothman DL. Proposed cycles for functional glutamate trafficking in synaptic neurotransmission. Neurochem. Int. 2008; 52(4–5): 809–825.
43. DiNuzzo M, Mangia S, Maraviglia B, Giove F. Changes in glucose uptake rather than lactate shuttle take center stage in subserving neuroenergetics: evidence from mathematical modeling. J. Cereb. Blood Flow Metab. 2010; 30(3): 586–602.
44. Shestov AA, Valette J, Uğurbil K, Henry P-G. On the reliability of (13)C metabolic modeling with two-compartment neuronal–glial models. J. Neurosci. Res. 2007; 85(15): 3294–3303.
45. Mason GF, Gruetter R, Rothman DL, Behar KL, Shulman RG, Novotny EJ. Simultaneous determination of the rates of the TCA cycle, glucose utilization, alpha-ketoglutarate/glutamate exchange, and glutamine synthesis in human brain by NMR. J. Cereb. Blood Flow Metab. 1995; 15(1): 12–25.
46. Yang J, Xu S, Shen J. Fast isotopic exchange between mitochondria and cytosol in brain revealed by relayed ^{13}C magnetization transfer spectroscopy. J. Cereb. Blood Flow Metab. 2009; 29(4): 661–669.
47. Shen J, Rothman D, Behar K, Xu S. Determination of the glutamate–glutamine cycling flux using two-compartment dynamic metabolic modeling is sensitive to astroglial dilution. J. Cereb. Blood Flow Metab. 2008; 29: 108–118.
48. McKenna MC. The glutamate–glutamine cycle is not stoichiometric: fates of glutamate in brain. J. Neurosci. Res. 2007; 85(15): 3347–3358.
49. Behar KL, Petroff OA, Prichard JW, Alger JR, Shulman RG. Detection of metabolites in rabbit brain by ^{13}C NMR spectroscopy following administration of [1-^{13}C]glucose. Magn. Reson. Med. 1986; 3(6): 911–920.
50. Fitzpatrick SM, Hetherington HP, Behar KL, Shulman RG. The flux from glucose to glutamate in the rat brain in vivo as determined by ^{1}H-observed, ^{13}C-edited NMR spectroscopy. J. Cereb. Blood Flow Metab. 1990; 10(2): 170–179.
51. Rothman DL, Behar KL, Hetherington HP, den Hollander JA, Bendall MR, Petroff OA, Shulman RG. ^{1}H-Observe/^{13}C-decouple spectroscopic measurements of lactate and glutamate in the rat brain in vivo. Proc. Natl. Acad. Sci. USA, 1985; 82(6): 1633–1637.
52. Gruetter R. Automatic, localized in vivo adjustment of all first- and second-order shim coils. Magn. Reson. Med. 1993; 29(6): 804–811.
53. Beckmann N, Turkalj I, Seelig J, Keller U. ^{13}C NMR for the assessment of human brain glucose metabolism in vivo. Biochemistry, 1991; 30(26): 6362–6366.
54. Gruetter R, Novotny EJ, Boulware SD, Rothman DL, Mason GF, Shulman GI, Shulman RG, Tamborlane WV. Direct measurement of brain glucose concentrations in humans by ^{13}C NMR spectroscopy. Proc. Natl. Acad. Sci. USA, 1992; 89(3): 1109–1112.
55. Rothman DL, Novotny EJ, Shulman GI, Howseman AM, Petroff OA, Mason G, Nixon T, Hanstock CC, Prichard JW, Shulman RG. ^{1}H–[^{13}C] NMR measurements of [4-^{13}C]glutamate turnover in human brain. Proc. Natl. Acad. Sci. USA, 1992; 89(20): 9603–9606.
56. Mason GF, Pan JW, Chu WJ, Newcomer BR, Zhang Y, Orr R, Hetherington HP. Measurement of the tricarboxylic acid cycle rate in human grey and white matter in vivo by ^{1}H–[^{13}C] magnetic resonance spectroscopy at 4.1T. J. Cereb. Blood Flow Metab. 1999; 19(11): 1179–1188.
57. Pan JW, Stein DT, Telang F, Lee JH, Shen J, Brown P, Cline G, Mason GF, Shulman GI, Rothman DL, Hetherington HP. Spectroscopic imaging of glutamate C4 turnover in human brain. Magn. Reson. Med. 2000; 44(5): 673–679.
58. Gruetter R, Seaquist ER, Kim S, Ugurbil K. Localized in vivo ^{13}C-NMR of glutamate metabolism in the human brain: initial results at 4 tesla. Dev. Neurosci. 1998; 20(4–5): 380–388.
59. van Eijsden P, Behar KL, Mason GF, Braun KPJ, de Graaf RA. In vivo neurochemical profiling of rat brain by ^{1}H–[^{13}C] NMR spectroscopy: cerebral energetics and glutamatergic/GABAergic neurotransmission. J. Neurochem. 2010; 112(1): 24–33.
60. Shulman RG, Rothman DL. Interpreting functional imaging studies in terms of neurotransmitter cycling. Proc. Natl. Acad. Sci. USA, 1998; 95(20): 11 993–11 998.

61. Raichle ME. A paradigm shift in functional brain imaging. J. Neurosci. 2009; 29(41): 12 729–12 734.
62. Owen OE, Morgan AP, Kemp HG, Sullivan JM, Herrera MG, Cahill GF. Brain metabolism during fasting. J. Clin. Invest. 1967; 46(10): 1589–1595.
63. van Hall G, Strømstad M, Rasmussen P, Jans O, Zaar M, Gam C, Quistorff B, Secher NH, Nielsen HB. Blood lactate is an important energy source for the human brain. J. Cereb. Blood Flow Metab. 2009; 29(6): 1121–1129.
64. Smith D, Pernet A, Hallett WA, Bingham E, Marsden PK, Amiel SA. Lactate: a preferred fuel for human brain metabolism in vivo. J. Cereb. Blood Flow Metab. 2003; 23(6): 658–664.
65. Gruetter R, Novotny EJ, Boulware SD, Rothman DL, Shulman RG. ^{1}H NMR studies of glucose transport in the human brain. J. Cereb. Blood Flow Metab. 1996; 16(3): 427–438.
66. Blomqvist G, Gjedde A, Gutniak M, Grill V, Widén L, Stone-Elander S, Hellstrand E. Facilitated transport of glucose from blood to brain in man and the effect of moderate hypoglycaemia on cerebral glucose utilization. Eur. J. Nucl. Med. 1991; 18(10): 834–837.
67. Heiss WD, Pawlik G, Herholz K, Wagner R, Göldner H, Wienhard K. Regional kinetic constants and cerebral metabolic rate for glucose in normal human volunteers determined by dynamic positron emission tomography of [^{18}F]-2-fluoro-2-deoxy-D-glucose. J. Cereb. Blood Flow Metab. 1984; 4(2): 212–223.
68. de Graaf RA, Pan JW, Telang F, Lee JH, Brown P, Novotny EJ, Hetherington HP, Rothman DL. Differentiation of glucose transport in human brain gray and white matter. J. Cereb. Blood Flow Metab. 2001; 21(5): 483–492.
69. Gruetter R, Ugurbil K, Seaquist ER. Steady-state cerebral glucose concentrations and transport in the human brain. J. Neurochem. 1998; 70(1): 397–408.
70. Simpson IA, Carruthers A, Vannucci SJ. Supply and demand in cerebral energy metabolism: the role of nutrient transporters. J. Cereb. Blood Flow Metab. 2007; 27(11): 1766–1791.
71. Badar-Goffer RS, Bachelard HS, Morris PG. Cerebral metabolism of acetate and glucose studied by ^{13}C-n.m.r. spectroscopy. A technique for investigating metabolic compartmentation in the brain. Biochem. J. 1990; 266(1): 133–139.
72. Cerdán S, Künnecke B, Seelig J. Cerebral metabolism of [1,2-^{13}C2]acetate as detected by in vivo and in vitro ^{13}C NMR. J. Biol. Chem. 1990; 265(22): 12 916–12 926.
73. Künnecke B, Cerdan S. Multilabeled ^{13}C substrates as probes in in vivo ^{13}C and ^{1}H NMR spectroscopy. NMR Biomed. 1989; 2(5–6): 274–277.
74. Waniewski RA, Martin DL. Preferential utilization of acetate by astrocytes is attributable to transport. J. Neurosci. 1998; 18(14): 5225–5233.
75. Blüml S, Moreno-Torres A, Shic F, Nguy C-H, Ross BD. Tricarboxylic acid cycle of glia in the in vivo human brain. NMR Biomed. 2002; 15(1): 1–5.
76. Mason GF, Petersen KF, Lebon V, Rothman DL, Shulman GI. Increased brain monocarboxylic acid transport and utilization in type 1 diabetes. Diabetes, 2006; 55(4): 929–934.
77. Pan JW, de Graaf RA, Petersen KF, Shulman GI, Hetherington HP, Rothman DL. [2,4-^{13}C2]-beta-Hydroxybutyrate metabolism in human brain. J. Cereb. Blood Flow Metab. 2002; 22(7): 890–898.
78. Boumezbeur F, Petersen KF, Cline GW, Mason GF, Behar KL, Shulman GI, Rothman DL. The contribution of blood lactate to brain energy metabolism in humans measured by dynamic ^{13}C nuclear magnetic resonance spectroscopy. J. Neurosci. 2010; 30(42): 13 983–13 991.
79. de Graaf RA. *In vivo NMR Spectroscopy*. Principles and Techniques: Wiley, Chichester, England; 2007.
80. Fox PT, Raichle ME, Mintun MA, Dence C. Nonoxidative glucose consumption during focal physiologic neural activity. Science, 1988; 241(4864): 462–464.
81. Dienel GA, Hertz L. Glucose and lactate metabolism during brain activation. J. Neurosci. Res. 2001; 66(5): 824–838.
82. Mangia S, Tkác I, Gruetter R, Van De Moortele P-F, Maraviglia B, Uğurbil K. Sustained neuronal activation raises oxidative metabolism to a new steady-state level: evidence from ^{1}H NMR spectroscopy in the human visual cortex. J. Cereb. Blood Flow Metab. 2007; 27(5): 1055–1063.
83. Prichard J, Rothman D, Novotny E, Petroff O, Kuwabara T, Avison M, Howseman A, Hanstock C, Shulman R. Lactate rise detected by ^{1}H NMR in human visual cortex during physiologic stimulation. Proc. Natl. Acad. Sci. USA, 1991; 88(13): 5829–5831.
84. Chen W, Zhu XH, Gruetter R, Seaquist ER, Adriany G, Ugurbil K. Study of tricarboxylic acid cycle flux changes in human visual cortex during hemifield visual stimulation using (1)H–[(13)C] MRS and fMRI. Magn. Reson. Med. 2001; 45(3): 349–355.
85. Hoge RD, Atkinson J, Gill B, Crelier GR, Marrett S, Pike GB. Linear coupling between cerebral blood flow and oxygen consumption in activated human cortex. Proc. Natl. Acad. Sci. USA, 1999; 96(16): 9403–9408.
86. Kim SG, Rostrup E, Larsson HB, Ogawa S, Paulson OB. Determination of relative CMRO2 from CBF and BOLD changes: significant increase of oxygen consumption rate during visual stimulation. Magn. Reson. Med. 1999; 41(6): 1152–1161.
87. Marrett S, Gjedde A. Changes of blood flow and oxygen consumption in visual cortex of living humans. Adv. Exp. Med. Biol. 1997; 413: 205–208.
88. Haga KK, Khor YP, Farrall A, Wardlaw JM. A systematic review of brain metabolite changes, measured with ^{1}H magnetic resonance spectroscopy, in healthy aging. Neurobiol. Aging, 2009; 30(3): 353–363.
89. Dager SR, Friedman SD, Parow A, Demopulos C, Stoll AL, Lyoo IK, Dunner DL, Renshaw PF. Brain metabolic alterations in medication-free patients with bipolar disorder. Arch. Gen. Psychiatry, 2004; 61(5): 450–458.
90. Sanacora G, Gueorguieva R, Epperson CN, Wu Y-T, Appel M, Rothman DL, Krystal JH, Mason GF. Subtype-specific alterations of gamma-aminobutyric acid and glutamate in patients with major depression. Arch. Gen. Psychiatry, 2004; 61(7): 705–713.
91. Gruber S, Frey R, Mlynárik V, Stadlbauer A, Heiden A, Kasper S, Kemp GJ, Moser E. Quantification of metabolic differences in the frontal brain of depressive patients and controls obtained by ^{1}H-MRS at 3 Tesla. Invest. Radiol. 2003; 38(7): 403–408.
92. Epperson CN, Haga K, Mason GF, Sellers E, Gueorguieva R, Zhang W, Weiss E, Rothman DL, Krystal JH. Cortical gamma-aminobutyric acid levels across the menstrual cycle in healthy women and those with premenstrual dysphoric disorder: a proton magnetic resonance spectroscopy study. Arch. Gen. Psychiatry, 2002; 59(9): 851–858.
93. Goddard AW, Mason GF, Almai A, Rothman DL, Behar KL, Petroff OA, Charney DS, Krystal JH. Reductions in occipital cortex GABA levels in panic disorder detected with ^{1}H-magnetic resonance spectroscopy. Arch. Gen. Psychiatry, 2001; 58(6): 556–561.
94. Hasler G, van der Veen JW, Tumonis T, Meyers N, Shen J, Drevets WC. Reduced prefrontal glutamate/glutamine and gamma-aminobutyric acid levels in major depression determined using proton magnetic resonance spectroscopy. Arch. Gen. Psychiatry, 2007; 64(2): 193–200.
95. Kuzniecky R, Ho S, Pan J, Martin R, Gilliam F, Faught E, Hetherington H. Modulation of cerebral GABA by topiramate, lamotrigine, and gabapentin in healthy adults. Neurology, 2002; 58(3): 368–372.
96. Novotny EJ, Hyder F, Shevell M, Rothman DL. GABA changes with vigabatrin in the developing human brain. Epilepsia, 1999; 40(4): 462–466.
97. Petroff OA, Mattson RH, Rothman DL. Proton MRS: GABA and glutamate. Adv. Neurol. 2000; 83: 261–271.
98. Novotny EJ, Fulbright RK, Pearl PL, Gibson KM, Rothman DL. Magnetic resonance spectroscopy of neurotransmitters in human brain. Ann. Neurol. 2003; 54 (Suppl 6): S25–S31.
99. Ross BD, Jacobson S, Villamil F, Korula J, Kreis R, Ernst T, Shonk T, Moats RA. Subclinical hepatic encephalopathy: proton MR spectroscopic abnormalities. Radiology, 1994; 193(2): 457–463.
100. Martin WRW. MR spectroscopy in neurodegenerative disease. Mol. Imaging Biol. 2007; 9(4): 196–203.
101. Ross B, Lin A, Harris K, Bhattacharya P, Schweinsburg B. Clinical experience with ^{13}C MRS in vivo. NMR Biomed. 2003; 16(6–7): 358–369.
102. Novotny EJ, Ogino T, Rothman DL, Petroff OA, Prichard JW, Shulman RG. Direct carbon versus proton heteronuclear editing of 2-^{13}C ethanol in rabbit brain in vivo: a sensitivity comparison. Magn. Reson. Med. 1990; 16(3): 431–443.
103. Rothman DL, Howseman AM, Graham GD, Petroff OA, Lantos G, Fayad PB, Brass LM, Shulman GI, Shulman RG, Prichard JW. Localized proton NMR observation of [3-^{13}C]lactate in stroke after [1-^{13}C]glucose infusion. Magn. Reson. Med. 1991; 21(2): 302–307.
104. Petroff OA, Graham GD, Blamire AM, al-Rayess M, Rothman DL, Fayad PB, Brass LM, Shulman RG, Prichard JW. Spectroscopic

imaging of stroke in humans: histopathology correlates of spectral changes. Neurology, 1992; 42(7): 1349–1354.
105. Terpstra M, Gruetter R, High WB, Mescher M, DelaBarre L, Merkle H, Garwood M. Lactate turnover in rat glioma measured by in vivo nuclear magnetic resonance spectroscopy. Cancer Res. 1998; 58(22): 5083–5088.
106. Wijnen JP, van der Graaf M, Scheenen TWJ, Klomp DWJ, de Galan BE, Idema AJS, Heerschap A. In vivo ^{13}C magnetic resonance spectroscopy of a human brain tumor after application of ^{13}C-1-enriched glucose. Magn. Reson. Imaging, 2010; 28(5): 690–697.
107. Butterworth RF. Portal-systemic encephalopathy: a disorder of neuron-astrocytic metabolic trafficking. Dev. Neurosci. 1993; 15 (3–5): 313–319.
108. Behar KL, Rothman DL, Petersen KF, Hooten M, Delaney R, Petroff OA, Shulman GI, Navarro V, Petrakis IL, Charney DS, Krystal JH. Preliminary evidence of low cortical GABA levels in localized ^{1}H-MR spectra of alcohol-dependent and hepatic encephalopathy patients. Am. J. Psychiatry, 1999; 156(6): 952–954.
109. Fitzpatrick SM, Hetherington HP, Behar KL, Shulman RG. Effects of acute hyperammonemia on cerebral amino acid metabolism and pHi in vivo, measured by ^{1}H and ^{31}P nuclear magnetic resonance. J. Neurochem. 1989; 52(3): 741–749.
110. Kanamori K, Ross BD. Glial alkalinization detected in vivo by ^{1}H–^{15}N heteronuclear multiple-quantum coherence-transfer NMR in severely hyperammonemic rat. J. Neurochem. 1997; 68(3): 1209–1220.
111. Behar KL, Fitzpatrick SM. Effects of hypercarbia and porta-caval shunting on amino acids and high energy phosphates of the rat brain: a ^{1}H and ^{31}P NMR study. In: Butterworth RF, Layrargues GP (eds.). *Hepatic Encephalopathy, Pathophysiology and Treatment*. Humana Press: Clifton, NJ; 1989, pp. 189–200.
112. Fitzpatrick SM, Behar KL, Shulman RG. In vivo NMR spectroscopy studies of cerebral metabolism in rats after portal–caval shunting. In: Butterworth RF, Layrargues GP (eds.). *Hepatic Encephalopathy, Pathophysiology and Treatment*. Humana Press: Clifton, NJ; 1989, pp. 177–187.
113. Blüml S, Moreno-Torres A, Ross BD. [1-^{13}C]glucose MRS in chronic hepatic encephalopathy in man. Magn. Reson. Med. 2001; 45(6): 981–993.
114. Gropman AL, Sailasuta N, Harris KC, Abulseoud O, Ross BD. Ornithine transcarbamylase deficiency with persistent abnormality in cerebral glutamate metabolism in adults. Radiology, 2009; 252(3): 833–841.
115. Lin MT, Beal MF. Mitochondrial dysfunction and oxidative stress in neurodegenerative diseases. Nature, 2006; 443(7113): 787–795.
116. Kalpouzos G, Chételat G, Baron J-C, Landeau B, Mevel K, Godeau C, Barré L, Constans J-M, Viader F, Eustache F, Desgranges B. Voxel-based mapping of brain gray matter volume and glucose metabolism profiles in normal aging. Neurobiol. Aging, 2009; 30(1): 112–124.
117. Rapoport SI. Functional brain imaging in the resting state and during activation in Alzheimer's disease. Implications for disease mechanisms involving oxidative phosphorylation. Ann. NY Acad. Sci. 1999; 893: 138–153.
118. Lin AP, Shic F, Enriquez C, Ross BD. Reduced glutamate neurotransmission in patients with Alzheimer's disease – an in vivo (13)C magnetic resonance spectroscopy study. MAGMA, 2003; 16(1): 29–42.
119. Cryer PE. Diverse causes of hypoglycemia-associated autonomic failure in diabetes. N. Engl. J. Med. 2004; 350(22): 2272–2279.
120. Cryer PE. Banting Lecture. Hypoglycemia: the limiting factor in the management of IDDM. Diabetes, 1994; 43(11): 1378–1389.
121. Oz G, Kumar A, Rao JP, Kodl CT, Chow L, Eberly LE, Seaquist ER. Human brain glycogen metabolism during and after hypoglycemia. Diabetes, 2009; 58(9): 1978–1985.
122. Pan JW, Williamson A, Cavus I, Hetherington HP, Zaveri H, Petroff OAC, Spencer DD. Neurometabolism in human epilepsy. Epilepsia, 2008; 49 (Suppl 3): 31–41.
123. Cavus I, Kasoff WS, Cassaday MP, Jacob R, Gueorguieva R, Sherwin RS, Krystal JH, Spencer DD, Abi-Saab WM. Extracellular metabolites in the cortex and hippocampus of epileptic patients. Ann. Neurol. 2005; 57(2): 226–235.
124. Petroff OAC, Errante LD, Rothman DL, Kim JH, Spencer DD. Glutamate–glutamine cycling in the epileptic human hippocampus. Epilepsia, 2002; 43(7): 703–710.
125. Eid T, Thomas MJ, Spencer DD, Rundén-Pran E, Lai JCK, Malthankar GV, Kim JH, Danbolt NC, Ottersen OP, de Lanerolle NC. Loss of glutamine synthetase in the human epileptogenic hippocampus: possible mechanism for raised extracellular glutamate in mesial temporal lobe epilepsy. Lancet, 2004; 363(9402): 28–37.
126. Blüml S, Moreno A, Hwang JH, Ross BD. 1-(13)C glucose magnetic resonance spectroscopy of pediatric and adult brain disorders. NMR Biomed. 2001; 14(1): 19–32.
127. de Graaf RA, Mason GF, Patel AB, Rothman DL, Behar KL. Regional glucose metabolism and glutamatergic neurotransmission in rat brain in vivo. Proc. Natl. Acad. Sci. USA, 2004; 101(34): 12 700–12 705.
128. Pfeuffer J, Tkác I, Choi IY, Merkle H, Ugurbil K, Garwood M, Gruetter R. Localized in vivo ^{1}H NMR detection of neurotransmitter labeling in rat brain during infusion of [1-^{13}C] D-glucose. Magn. Reson. Med. 1999; 41(6): 1077–1083.
129. Cudalbu C, Comment A, Kurdzesau F, van Heeswijk RB, Uffmann K, Jannin S, Denisov V, Kirik D, Gruetter R. Feasibility of in vivo ^{15}N MRS detection of hyperpolarized ^{15}N labeled choline in rats. Phys. Chem. Chem. Phys. 2010; 12(22): 5818–5823.
130. Marjańska M, Iltis I, Shestov AA, Deelchand DK, Nelson C, Uğurbil K, Henry P-G. In vivo ^{13}C spectroscopy in the rat brain using hyperpolarized [1-(13)C]pyruvate and [2-(13)C]pyruvate. J. Magn. Reson. 2010; 206(2): 210–218.
131. Bhattacharya P, Chekmenev EY, Perman WH, Harris KC, Lin AP, Norton VA, Tan CT, Ross BD, Weitekamp DP. Towards hyperpolarized (13)C-succinate imaging of brain cancer. J. Magn. Reson. 2007; 186(1): 150–155.
132. Hetherington HP, Chu W-J, Gonen O, Pan JW. Robust fully automated shimming of the human brain for high-field ^{1}H spectroscopic imaging. Magn. Reson. Med. 2006; 56(1): 26–33.
133. Juchem C, Nixon TW, McIntyre S, Rothman DL, de Graaf RA. Magnetic field homogenization of the human prefrontal cortex with a set of localized electrical coils. Magn. Reson. Med. 2010; 63(1): 171–180.
134. Koch KM, Sacolick LI, Nixon TW, McIntyre S, Rothman DL, de Graaf RA. Dynamically shimmed multivoxel ^{1}H magnetic resonance spectroscopy and multislice magnetic resonance spectroscopic imaging of the human brain. Magn. Reson. Med. 2007; 57(3): 587–591.
135. de Graaf RA. Theoretical and experimental evaluation of broadband decoupling techniques for in vivo nuclear magnetic resonance spectroscopy. Magn. Reson. Med. 2005; 53(6): 1297–1306.
136. Collins CM, Liu W, Wang J, Gruetter R, Vaughan JT, Ugurbil K, Smith MB. Temperature and SAR calculations for a human head within volume and surface coils at 64 and 300 MHz. J. Magn. Reson. Imaging, 2004; 19(5): 650–656.
137. Adriany G, Gruetter R. A half-volume coil for efficient proton decoupling in humans at 4 tesla. J. Magn. Reson. 1997; 125(1): 178–184.
138. Klomp DWJ, Renema WKJ, van der Graaf M, de Galan BE, Kentgens APM, Heerschap A. Sensitivity-enhanced ^{13}C MR spectroscopy of the human brain at 3 Tesla. Magn. Reson. Med. 2006; 55(2): 271–278.
139. Li S, Yang J, Shen J. Novel strategy for cerebral ^{13}C MRS using very low RF power for proton decoupling. Magn. Reson. Med. 2007; 57(2): 265–271.
140. Sailasuta N, Abulseoud O, Harris KC, Ross BD. Glial dysfunction in abstinent methamphetamine abusers. J. Cereb. Blood Flow Metab. 2010; 30(5): 950–960.
141. Li S, Zhang Y, Wang S, Yang J, Ferraris Araneta M, Farris A, Johnson C, Fox S, Innis R, Shen J. In vivo ^{13}C magnetic resonance spectroscopy of human brain on a clinical 3 T scanner using [2-^{13} C]glucose infusion and low-power stochastic decoupling. Magn. Reson. Med. 2009; 62(3): 565–573.
142. Li S, Zhang Y, Wang S, Araneta MF, Johnson CS, Xiang Y, Innis RB, Shen J. ^{13} C MRS of occipital and frontal lobes at 3 T using a volume coil for stochastic proton decoupling. NMR Biomed. 2010; 23(8): 977–985.
143. Mason GF, Rothman DL. Basic principles of metabolic modeling of NMR (13)C isotopic turnover to determine rates of brain metabolism in vivo. Metab. Eng. 2004; 6(1): 75–84.
144. Moreno A, Blüml S, Hwang JH, Ross BD. Alternative 1-(13)C glucose infusion protocols for clinical (13)C MRS examinations of the brain. Magn. Reson. Med. 2001; 46(1): 39–48.
145. Mason GF, Falk Petersen K, de Graaf RA, Kanamatsu T, Otsuki T, Shulman GI, Rothman DL. A comparison of (13)C NMR measurements of the rates of glutamine synthesis and the tricarboxylic acid cycle during oral and intravenous administration of [1-(13)C]glucose. Brain Res. Brain Res. Protoc. 2003; 10(3): 181–190.
146. van de Ven KCC, van der Graaf M, Tack CJJ, Klomp DWJ, Heerschap A, de Galan BE. Optimized [1-(13)C]glucose infusion protocol for ^{13}C

magnetic resonance spectroscopy at 3T of human brain glucose metabolism under euglycemic and hypoglycemic conditions. J. Neurosci. Methods, 2010; 186(1): 68–71.
147. Sailasuta N, Tran TT, Harris KC, Ross BD. Swift Acetate Glial Assay (SAGA): an accelerated human (13)C MRS brain exam for clinical diagnostic use. J. Magn. Reson. 2010; 207(2): 352–355.
148. Chhina N, Kuestermann E, Halliday J, Simpson LJ, Macdonald IA, Bachelard HS, Morris PG. Measurement of human tricarboxylic acid cycle rates during visual activation by (13)C magnetic resonance spectroscopy. J. Neurosci. Res. 2001; 66(5): 737–746.
149. Henry P-G, Criego AB, Kumar A, Seaquist ER. Measurement of cerebral oxidative glucose consumption in patients with type 1 diabetes mellitus and hypoglycemia unawareness using (13)C nuclear magnetic resonance spectroscopy. Metab. Clin. Exp. 2010; 59(1): 100–106.
150. Patel AB, de Graaf RA, Mason GF, Kanamatsu T, Rothman DL, Shulman RG, Behar KL. Glutamatergic neurotransmission and neuronal glucose oxidation are coupled during intense neuronal activation. J. Cereb. Blood Flow Metab. 2004; 24(9): 972–985.
151. Choi I-Y, Lei H, Gruetter R. Effect of deep pentobarbital anesthesia on neurotransmitter metabolism in vivo: on the correlation of total glucose consumption with glutamatergic action. J. Cereb. Blood Flow Metab. 2002; 22(11): 1343–1351.
152. Wang J, Jiang L, Jiang Y, Ma X, Chowdhury GMI, Mason GF. Regional metabolite levels and turnover in the awake rat brain under the influence of nicotine. J. Neurochem. 2010; 113(6): 1447–1458.
153. Yang J, Shen J. In vivo evidence for reduced cortical glutamate–glutamine cycling in rats treated with the antidepressant/antipanic drug phenelzine. Neuroscience, 2005; 135(3): 927–937.